Molecular Crystals and Liquid Crystals

Publication details, including instructions for authors and subscription information:
http://www.tandfonline.com/loi/gmcl20

Supramolecular Hydrogen-Bonded Liquid Crystals Formed from 4-(4′-Pyridylazophenyl)-4″-alkoxy Benzoates and 4-Substituted Benzoic Acids

M. M. Naoum [a], A. A. Fahmi [a] & M. A. Alaasar [a]

[a] Department of Chemistry, Faculty of Science, Cairo University, Cairo, Egypt

Version of record first published: 31 Aug 2012.

To cite this article: M. M. Naoum , A. A. Fahmi & M. A. Alaasar (2008): Supramolecular Hydrogen-Bonded Liquid Crystals Formed from 4-(4′-Pyridylazophenyl)-4″-alkoxy Benzoates and 4-Substituted Benzoic Acids, Molecular Crystals and Liquid Crystals, 487:1, 74-91

To link to this article: http://dx.doi.org/10.1080/15421400802198631

Mol. Cryst. Liq. Cryst., Vol. 487, pp. 74–91, 2008

ISSN: 1542-1406 print/1563-5287 online
DOI: 10.1080/15421400802198631

Taylor & Francis
Taylor & Francis Group

Supramolecular Hydrogen-Bonded Liquid Crystals Formed from 4-(4′-Pyridylazophenyl)-4″-alkoxy Benzoates and 4-Substituted Benzoic Acids

M. M. Naoum, A. A. Fahmi, and M. A. Alaasar
Department of Chemistry, Faculty of Science, Cairo University, Cairo, Egypt

*Four pyridine-based derivatives (***I**10*, **I**12*, **I**14*, and **I**18*) with molecular formula $C_nH_{2n+1}O$-$C_6H_4COOC_6H_4$-N=N-C_5H_4N, that differ from each other in the number of carbon atoms, n, were prepared and characterized for their mesophase behavior. The number of carbons in the alkoxy chain varies between 10, 12, 14, to 18 atoms, respectively. Liquid crystalline properties were studied for two series of hydrogen-bonded liquid crystal complexes, consisting of the central 4-pyridylazophenyl benzoate and substituted benzoic acids. In the first series of the supramolecular complexes (group* **A***), the lengths of the alkoxy chains on both of the azo pyridine and the benzoic acid components have varied between 10, 12, 14, and 18 carbons. In the second series (group* **B***), the same proton-acceptors, i.e., the pyridyl azo derivatives, were used but with benzoic acids* para*-substituted with small compact polar groups, X. All of the newly prepared pyridine-based derivatives and their hydrogen-bonded complexes were found to be mesomorphic. The newly prepared pyridine-based derivatives and their supramolecular complexes in both groups were characterized for their mesophase behavior by differential scanning calorimetry, DSC, and polarized light microscopy, PLM. Four 4-alkoxybenzoic acids ($C_mH_{2m+1}OC_6H_4COOH$,* **II**10*,* **II**12*,* **II**14*, and* **II**18*) were used in group* **A** *series; the number of carbons (m) of their alkoxy groups also varies between 10, 12, 14, and 18, respectively. Substituents on the other group of acids (*$\mathbf{III}_{a-f}$*) in group* **B** *series vary, respectively, between CH_3O, CH_3, H, Br, CN, and NO_2. Smectic C mesophase is induced in most of the binary mixtures investigated.*

Keywords: 4-(4′-pyridylazophenyl)-4″-alkoxy benzoates; 4-substituted benzoic acids; supramolecular LCs

INTRODUCTION

Binary mixtures of liquid crystalline materials can often lead either to new liquid crystal phases, not observed in the corresponding pure

Address correspondence to M. M. Naoum, Department of Chemistry, Faculty of Science, Cairo University, Cairo, Egypt. E-mail: magdinaoum@yahoo.co.uk

systems, or to the extension of the temperature range over which their mesophases are stable [1,2]. The enhancement of the liquid crystalline region often occurs because of the depression in the melting point, which reaches a minimum at the eutectic composition. However, for certain materials, it is possible to observe, instead of melting point depression, liquid crystal phases that are formed via tailoring the molecular interaction between the components of the mixture, thus, increasing the stability of the induced mesophase, i.e., increasing the mesophase—isotropic transition temperature, $\boldsymbol{T}_{C}$ [3–7].

Supramolecular liquid crystals are frequently induced by hydrogen bonding between aromatic carboxylic acids as proton donor and pyridyl fragments as proton acceptors. In such cases, hydrogen bonding leads to an elongation of the rigid rod segment of the individual components, and, in this manner hydrogen-bonded liquid crystal complexes are obtained [8–10].

We have recently [11] reported the preparation and characterization of new liquid crystal materials based on supramolecular hydrogen-bonded complexes between 4-alkoxybenzoic acids (as the proton donor) and 4-(4′-pyridylazophenyl)-4″-substituted benzoates (as the proton-acceptors). The latter was designed in such a manner as to combine an azo, ester, and pyridine moieties in one and the same molecule. Although none of the therein investigated pyridine-based derivatives was mesomorphic [11], the long tail of the alkoxy group on the benzoic acid component furnishes complexes with rod-shaped assembly, and, consequently, the resulting supramolecular structures were found to be mesomorphic. Furthermore, the binary phase diagrams reported therein [11], revealed that the electron-donating substituent (CH_3O or CH_3), on the pyridine-based moiety, enhances the stability of the hydrogen-bond, and a complex is observed (in either the solid or the mesophase), irrespective of the length of the alkoxy-chain on the acid. These findings have encouraged us to extend our investigation to prepare, hopefully, pyridine-based liquid crystals via replacing the polar substituent (X) by an alkoxy group of varying chain length. This may, on one hand, render the derivative more or less mesomorphic, and on the other hand, lead to an increase of the electron-density on the pyridine nitrogen, due to its powerful electron-donating efficiency, as the CH_3O group did in our previous investigation [11].

The goal of the present study is, first, to prepare a new group of pyridine based derivatives (**I***10*, **I***12*, **I***14*, and **I***18*) bearing, this time, an alkoxy group with a number of carbon atoms varying between 10, 12, 14, and 18, respectively, and to investigate their phase behavior

via DSC and PLM. The second aim of this investigation is to rule out their ability towards supramolecular hydrogen-bond formation, individually, with two groups of benzoic acids. In the first, **II***10*, **II***12*, **II***14*, and **II***18*, the substituents are 4-alkoxy group with a number of carbon atoms varies between 10, 12, 14, and 18 carbons, respectively. In the second group of acids (**III**$_{a–f}$), the substituents X are of different polarity that changes between CH_3O, CH_3, H, Br, CN, and NO_2, respectively.

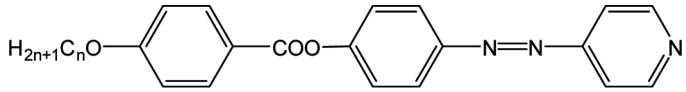

(**I***n*)

I*10*, n = 10, **I***12*, n = 12, **I***14*, n = 14, **I***18*, n = 18

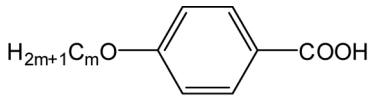

(**II***m*)

II*10*, *m*=10, **II***12*, *m*=12, **II***14*, *m*=14, **II***18*, *m*=18

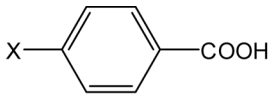

(**III**$_{a-f}$)

III$_a$, X= CH_3O, **III**$_b$, X= CH_3, **III**$_c$, X= H, **III**$_d$, X= Br, **III**$_e$, **X=** CN, **III**$_f$, X= NO_2

EXPERIMENTAL

Chemicals were purchased from the following Companies: Fluka, Buchs, Switzerland; MP Biomedicals, Inc., Illkirch, France; BDH, Poole, England; Aldrich, Wisconsin, USA; and E. Merck, Darmstadt, Germany.

Preparation of Materials

All benzoic acids (**II***10*–**II***18*) were prepared according to the methods described previously [12]. Transition temperatures of all acids, as given in Table 1, agreed with those reported before [10].

TABLE 1 Phase Transition Temperatures (°C) of the acids, **II***m*

Compound number	*m*	$T_{S\text{-}A}$	$T_{A\text{-}N}$	$T_{S\text{-}I}$	$T_{N\text{-}I}$
II*10*	10	101	122	–	141
II*12*	12	93	129	–	137
II*14*	14	89	–	133	–
II*18*	18	109	–	126	–

The pyridine-based azo dyes (**I***n*) were prepared according to the following scheme:

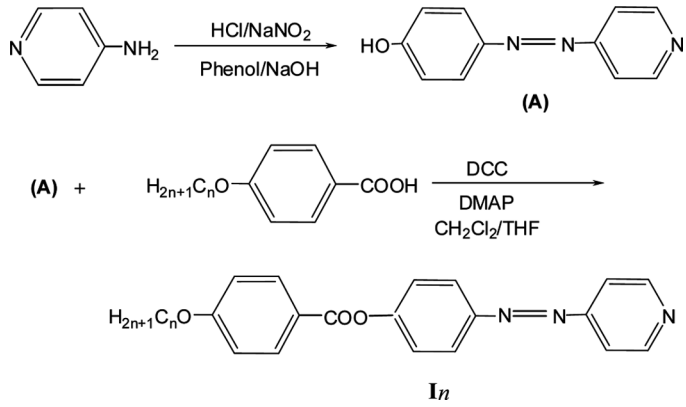

Preparation of 4-(4′-Pyridylazo)-Phenol (A)

This was prepared according to the method described by Zhang *et al.* [13] from 4-aminopyridine and phenol. To a solution of 4.0 g (0.058 mol) of sodium nitrite in 20 ml water, 5.0 g (0.053 mol) phenol in 45 ml of 10% sodium hydroxide solution (0.1125 mol) was added with stirring while cooling both solutions to 0°C. The resulting solution was added to a cooled solution of 4-aminopyridine (6.0 g, 0.064 mol) in 25 ml (0.25 mol) concentrated hydrochloric acid and 16 ml water with stirring for 10 minutes below 0°C. Subsequently, a saturated solution of sodium carbonate was added to adjust the pH of the mixture to about 6. A yellow dye is formed which was filtered off and used for subsequent steps without purification. The yield of the crude product was 75%.

*Preparation of 4-(4′-Pyridylazophenyl)-4″-alkoxy Benzoates (***I***10–***I***18)*

The azo A (0.60 g, 0.0027 mol) with its molar equivalent of the acid (**II***m*), 1.11 g (0.0054 mol) of DCC, and few crystals of the catalyst,

4-(dimethylamino) pyridine (DMAP), were dissolved in 100 ml (1:1) mixture of CH_2Cl_2 and THF; the mixture was left to stand, at room temperature with stirring, for at least 72 hrs. The solid was filtered off, washed with 20 ml CH_2Cl_2, and the filtrate allowed to evaporate. The residue was then soaked in methanol for 2 hrs with stirring and filtered. The solids (≈50% yield) obtained were found to be TLC pure and possess sharp transition temperatures as measured by DSC and are given in Table 2.

Confirmation of Molecular Structure

The molecular formulae of the newly prepared pyridine-based derivatives (**II***10*–**II***18*) were confirmed via elemental analyses, infrared, NMR, and mass spectroscopy. The results agreed, within the permissible limits, with the proposed structures.

Physical Characterization

Infrared absorption spectra were measured with a Perkin-Elmer B25 spectrophotometer, and ^{1}H-nmr spectra with a Varian EM 350L.

Calorimetric investigations were carried out using a PL-DSC of Polymer Laboratories, England. The instrument was calibrated for temperature, heat, and heat flow according to the method recommended by Cammenga *et al.* [14]. DSC measurements were carried out on small samples (2–3 mg) placed in sealed aluminum pans. All of the thermograms have been achieved at a heating rate of 10°C/min in inert atmosphere of nitrogen gas (10 ml/min).

Transition temperatures were checked and types of mesophases identified for mixtures prepared and their pure components with a

TABLE 2 Transition Temperatures (°C) and Transition Enthalpies of the Pyridine-Based Azo Dyes, **I***n*

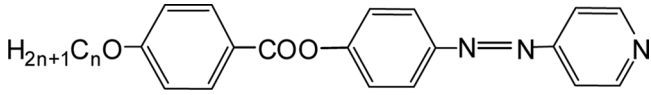

Compound number	*n*	T_m	ΔH_m (kJ/mol)	$T_{A\text{-}I}$	$\Delta H_{A\text{-}I}$ (kJ/mol)
I*10*	10	96.6	26.96	128.8	1.71
I*12*	12	104.2	43.72	135.8	4.87
I*14*	14	96.2	31.00	–	–
I*18*	18	99.0	29.72	119.5	2.98

standard polarized light microscope PLM (Wild, Germany) attached to a home made hot-stage.

Thin-layer chromatography was performed with TLC-sheets coated with silica gel (E. Merck), whereby spots were detected by a uv-lamp.

Supramolecular complexes in the 1:1 molar ratio of any two complimentary components were prepared by melting the appropriate amounts of each component, stirring to give an intimate blend, and then cooling with stirring to room temperature. The transition temperatures obtained for the prepared complexes, as measured by both DSC and PLM, agreed within 2–3°C. In the figures, constructed by plotting transition temperatures versus the alkoxy-chain length (n or m), the symbol "○" denotes solid-mesophase, "□" mesophase-isotropic transitions, $\boldsymbol{T}_C$, and "•" mesophase-another mesophase.

RESULTS & DISCUSSION

Infrared Absorption Spectra of Pyridine-Based Derivatives

Infrared Spectra of 4-(4′-Pyridylazophenyl)-4″-Substituted Benzoates (IV$_{a–e}$)

Infrared absorption bands of the previously [11] investigated pyridine based series **IV**$_{a–e}$, with their assignments are given in Table 3. It can be noted from the table that, due to the variation in the electronic nature of the substituent X, its mesomeric interaction with the ester C=O group, via the intervening phenylene ring, will be different. Thus, the electron withdrawing (Br or NO_2) group raises the C=O stretching frequency (1743.5 cm^{-1}) in $\mathbf{I}_d$ or $\mathbf{I}_e$. Conversely, the electron-releasing character of the CH_3O or CH_3 groups resulted in compounds that absorb at lower frequencies (1728 cm^{-1}). Similar conclusions were arrived at [12] for the 4-alkoxyphenyl-4-substituted benzoates, where the ester C=O absorptions occur at 1742 and 1729 cm^{-1}, for the nitro- and methoxy- substituted derivatives,

TABLE 3 Infrared Absorption Spectra of 4-(4′-Pyridylazophenyl)-4″-Substituted Benzoates (**IV**$_{a–e}$)

Compound	X	$\nu_{C\text{-}H\ aromatic}$	$\nu_{C=O}$	$\nu_{N=N}$	$\nu_{C\text{-}O\ ester}$	$\nu_{C\text{-}O\ ether}$	ν_{NO2}
IV$_a$	CH_3O	2920	1728	1585	1273	1207	–
IV$_b$	CH_3	2920	1747	1593	1273	1227	–
IV$_c$	H	2920	1728	1585	1269	1207	–
IV$_d$	Br	2916	1743	1582	1265	1223	–
IV$_e$	NO_2	2931	1697	–	1273	1234	1527 1342

respectively. That is, electron-withdrawing substituent in the first compound shifts the absorption to higher frequency; while conjugative interaction leads to lowering the absorption frequency in the later. Other absorption frequencies, as given in Table 3 are in consistency with the structures proposed.

*Infrared Spectra of 4-(4′-Pyridylazophenyl)-4″-alkoxy Benzoates (I*n*)*

The corresponding infrared absorption bands of the series **I***n* are given in Table 4. The nearly identical infrared spectra observed for the four homologues investigated revealed that the mesomeric shift of the ester C=O group attached to the 4-position with respect to the alkoxy group is not significantly affected by the change in the length of the alkoxy chain. Fore example, the C-H stretching frequency is centered, in all compounds of the series, at 2920 cm^{-1}, and the azo–N=N-band is located at 1585 cm^{-1}. The stretching frequency of the ester C-O and ether C-O linkages are always found in its proper area, at 1285, and 1211 cm^{-1}, respectively. Again, other ir-bands are found (Table 4) to confirm the structures proposed.

DSC Analyses

Trends in the mesophase-isotropic liquid transition temperatures ($\boldsymbol{T}_C$) of liquid crystalline compounds were rationalized in terms of molecular structure, even for subtle differences as in homologous series. Two types of terminal substituents may be utilized: the homologous series and the small compact polar type.

Generally, complementary components in a mixture employed in the formation of liquid crystals may be either mesomorphic or nonmesomorphic or both; however, novel liquid crystals can be obtained. Hydrogen bonding between the two components of the mixture leads to an elongation of the rigid-rod segment of the individual components

TABLE 4 Infrared Absorption Spectra of 4-(4′-Pyridylazophenyl)-4′-alkoxy Benzoates (**I***n*)

Compound	$\nu_{C\text{-}H\ aromatic}$	$\nu_{C=O}$	$\nu_{N=N}$	$\nu_{C\text{-}O\ ester}$	$\nu_{C\text{-}O\ ether}$
I*10*	2920	1724	1581	1285	1211
I*12*	2920	1728	1585	1285	1211
I*14*	2920	1728	1581	1285	1211
I*18*	2916	1736	1585	1288	1215

as represented, for our investigated systems, by formula **1**:

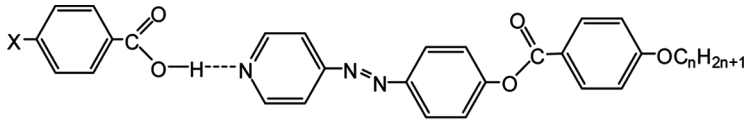

(1)

Transition temperatures of the investigated acids (**II***m*), as reported previously [10], are summarized in Table 1. Transition temperatures and transition enthalpies of pyridine-based derivatives (**I***n*) are given in Table 2. In these tables, the following symbols are used as subscripts to specify the various transition temperatures: solid (S), nematic (N), smectic A (A), smectic C (C), and isotropic (I). Transitions of solid to any liquid phase are also denoted as melting point ($\boldsymbol{T}_{\mathrm{m}}$), whereas the mesophase-isotropic transition also as clearing temperatures ($\boldsymbol{T}_{\mathrm{C}}$). It can be seen from the table that all of the pyridine based compounds investigated are of high melting ($\boldsymbol{T}_{\mathrm{m}}$) points, and all of them are mesomorphic.

In order to investigate the effect of the alkoxy-chain length, on the liquid crystalline properties of the supramolecular complexes of the type as given in Table 5 for group **A**, the number of carbons in the terminal alkoxy group on the pyridine-based derivatives was once kept constant at 10, 12, 14, and 18 atoms, while that on the acid complementary component was alternatively altered between 10 and 18 carbons. Figure 1 correlates the phase transition temperatures of each pyridine-based homologue with the alkoxy-chain length (m) of the acid. Alternatively, Fig. 2 reproduces the dependencies, on the chain length (*n*) of the pyridine-based component, of the phase transition temperature of 1:1 complex formed between each homologue of the acid and the different homologues of the pyridine-based derivatives.

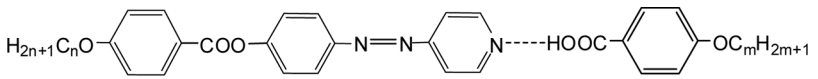

(Group ***A***)

As can be seen from both groups of figures, the Sm C mesophase is induced together with the Sm A phase in the lower homologues of either the proton donor (the acid) or proton-acceptor (the base). The temperature range of the Sm C mesophase increases on the expense of the Sm A phase so that it appears as the only mesophase for the highest homologue (m = 18), see Fig. 2d. It can also be noticed from the figures that the stability of the Sm C phase, i.e., $\boldsymbol{T}_{\mathrm{C\text{-}I}}$, decreases slightly with increase of the alkoxy-chain length on either

TABLE 5 Phase Transition Temperatures (°C) of the Supramolecular Complexes (Group A) Formed Between the Pyridine-Based Derivatives (**I***n*) and the 4-alkoxy Benzoic Acids (**II***m*)

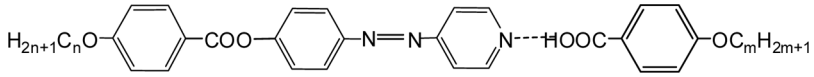

Base	Acid	$T_{S\text{-}A}$	$T_{S\text{-}C}$	$T_{A\text{-}C}$	$T_{A\text{-}I}$	$T_{C\text{-}I}$
I*10*	**II***10*	98.6	–	164.8	–	171.2
	II*12*	96.1	–	160.0	–	166.1
	II*14*	99.0	–	156.3	–	163.0
	II*18*	96.3	–	–	158.1	–
I*12*	**II***10*	96.9	–	163.6	–	171.9
	II*12*	102.0	–	163.1	–	172.0
	II*14*	101.1	–	158.2	–	168.1
	II*18*	99.9	–	158.0	–	161.9
I*14*	**II***10*	96.0	–	146.5	–	171.2
	II*12*	99.9	–	151.0	–	170.5
	II*14*	103.8	–	156.4	–	167.8
	II*18*	104.5	–	153.1	–	163.2
I*18*	**II***10*	–	96.4	–	–	166.1
	II*12*	–	101.9	–	–	164.6
	II*14*	–	105.6	–	–	159.6
	II*18*	–	111.6	–	–	158.0

components. On the other hand, the stability of the Sm A mesophase, i.e., $T_{A\text{-}C}$, decreases as the alkoxy-chain length of the pyridine-based constituent is lengthened and disappeared completely at $n = 18$. Furthermore, except for the lower homologues, the melting points, i.e., $T_{S\text{-}A}$ or $T_{S\text{-}C}$, are found to be regularly, but slightly, increased with the length of the alkoxy chain on either component.

Table 6 and Fig. 3 illustrate the dependences on the pyridine-based alkoxy-chain length (n) of transition temperatures of the supramolecular complexes (group ***B***) formed between the pyridine-based derivatives (**I***n*) and the substituted benzoic acids ($\mathbf{III}_{a-f}$).

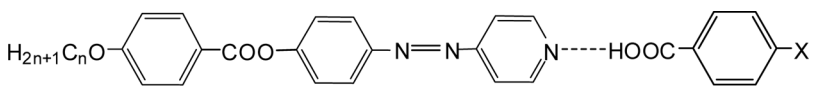

(Group ***B***)

As can be seen from Fig. 3, the electron-withdrawing substituent (Br, CN, or NO_2), on the acid segment of the supramolecular complex, induces a stable Sm C mesophase that covers a wide range

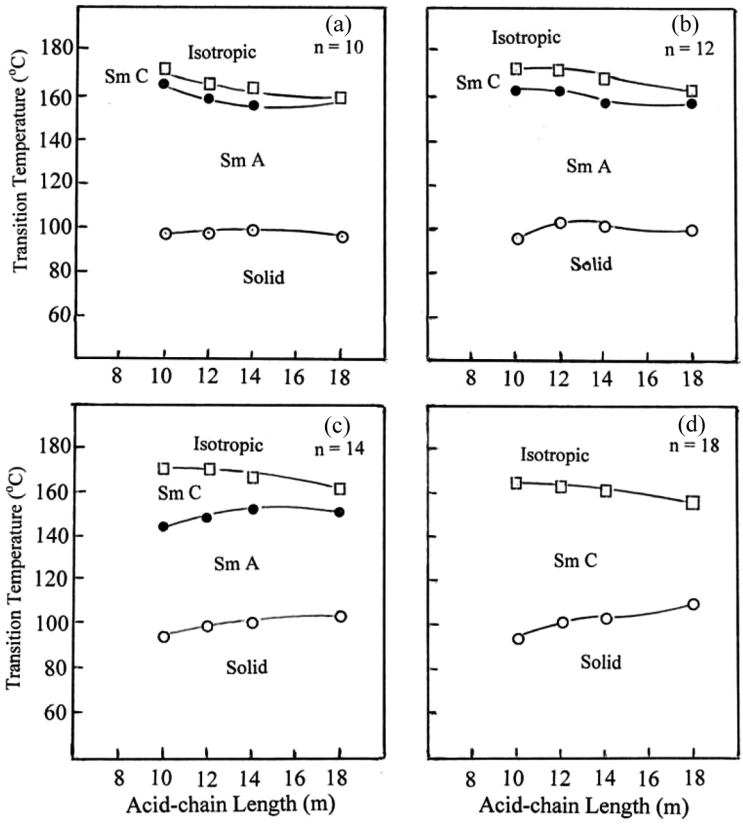

FIGURE 1 Effect of acid-chain length (m) on the transition temperature of the supra molecular complexes of Group ***A*** series, (a) $n = 10$, (b) $n = 12$, (c) $n = 14$, and (d) $n = 18$.

of temperatures and is independent of the length of the pyridine-based alkoxy chain. At the same time, the Sm A mesophase occupies a relatively small temperature range that precedes the Sm C phase. Conversely, the electron-donating (CH_3O or CH_3) substituted, as well as the unsubstituted acids, furnish complexes possessing mainly the Sm A mesophase with a small Sm C temperature range that disappeared completely in the complexes of the higher homologues of the base (i.e., when $n > 14$).

It is worthy here to compare the results of Group ***B*** with those of the previously [11] investigated series (group **C**), where the substituent X is interchanged with the alkoxy group.

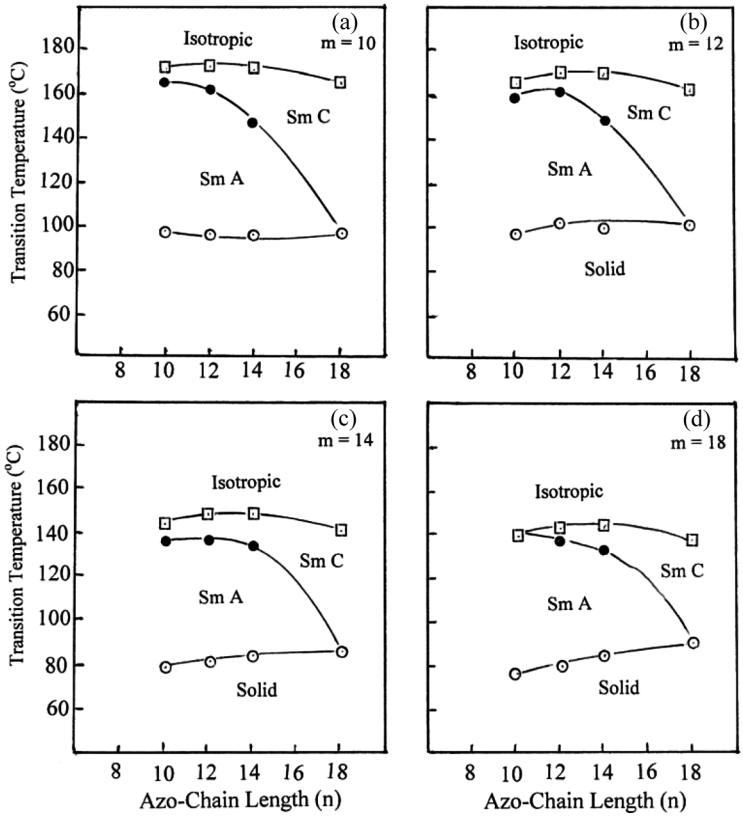

FIGURE 2 Effect of Azo-chain length (n) on the transition temperature of the supramolecular complexes of Group ***A*** series, (a) $m = 10$, (b) $m = 12$, (c) $m = 14$, and (d) $m = 18$.

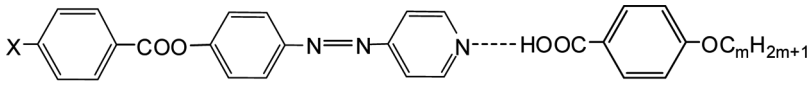

(Group ***C***)

The chain-length (m) dependencies of the transition temperatures of group ***C*** complexes are illustrated graphically in Fig. 4. In this group of complexes, it was observed that polar substitutents, in the pyridine-based component, are more or less pronounced in promoting the Sm C mesophase. Thus, each of the electron-withdrawing (Br or NO_2), electron-donating (CH_3O or CH_3), and the un-substituted pyridine-based derivatives is found to possess a considerable Sm C

TABLE 6 Phase Transition Temperatures (°C) of the Supramolecular Complexes (Group ***B***) Formed Between the Pyridine-Based Derivatives (**I***n*) and the 4-Substituted Benzoic Acids ($\mathbf{III}_{a-f}$)

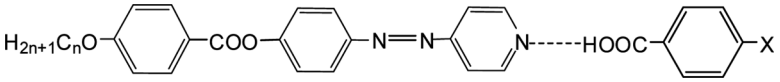

Acid	X	$\Delta\alpha_X \times 10^{24}$	Base	$T_{S\text{-}A}$	$T_{A\text{-}C}$	$T_{A\text{-}I}$	$T_{C\text{-}I}$
$\mathbf{III}_a$	CH_3O	3.86	**I***10*	83.9	152.6	–	163.7
			I*12*	95.6	157.8	–	161.1
			I*14*	98.2		155.8	–
			I*18*	96.1	–	155.4	–
$\mathbf{III}_b$	CH_3	2.12	**I***10*	80.4	164.1	–	188.3
			I*12*	85.5	163.1	–	168.3
			I*14*	84.5	–	161.9	–
			I*18*	82.4	–	156.5	–
	H	0.0	**I***10*	94.4	155.4	–	170.2
			I*12*	86.5	155.7	–	162.0
			I*14*	89.6	–	156.2	–
			I*18*	89.9	–	159.6	–
$\mathbf{III}_d$	Br	3.11	**I***10*	81.5	108.0	–	170.1
			I*12*	89.2	100.5	–	171.3
			I*14*	90.2	111.2	–	175.2
			I*18*	93.0	113.0	–	177.9
$\mathbf{III}_e$	CN	5.12	**I***10*	85.2	103.2	–	173.9
			I*12*	88.3	112.2	–	162.1
			I*14*	89.7	106.5	–	175.8
			I*18*	92.8	105.7	–	197.7
$\mathbf{III}_f$	NO_2	4.58	**I***10*	82.2	108.2	–	185.8
			I*12*	87.3	101.7	–	180.4
			I*14*	85.2	105.7	–	180.5
			I*18*	89.3	106.2	–	193.2

temperature range with all the investigated homologues of the acid (**II***m*). The Sm A phase appeared within a small temperature range in the case of the complexes formed between the CH_3O or CH_3-substituted base and the decyloxy ($m = 10$) benzoic acid. On the other hand, the nitro analog showed the Sm A phase with all homologues of the acid investigated.

Transition Temperature and Polarizability Anisotropy

Generally, the stability of a mesophase is greater, the greater the lateral adhesion of the rod-shaped molecules, which in turn, would be augmented by the increase in polarity and/or polarizability of

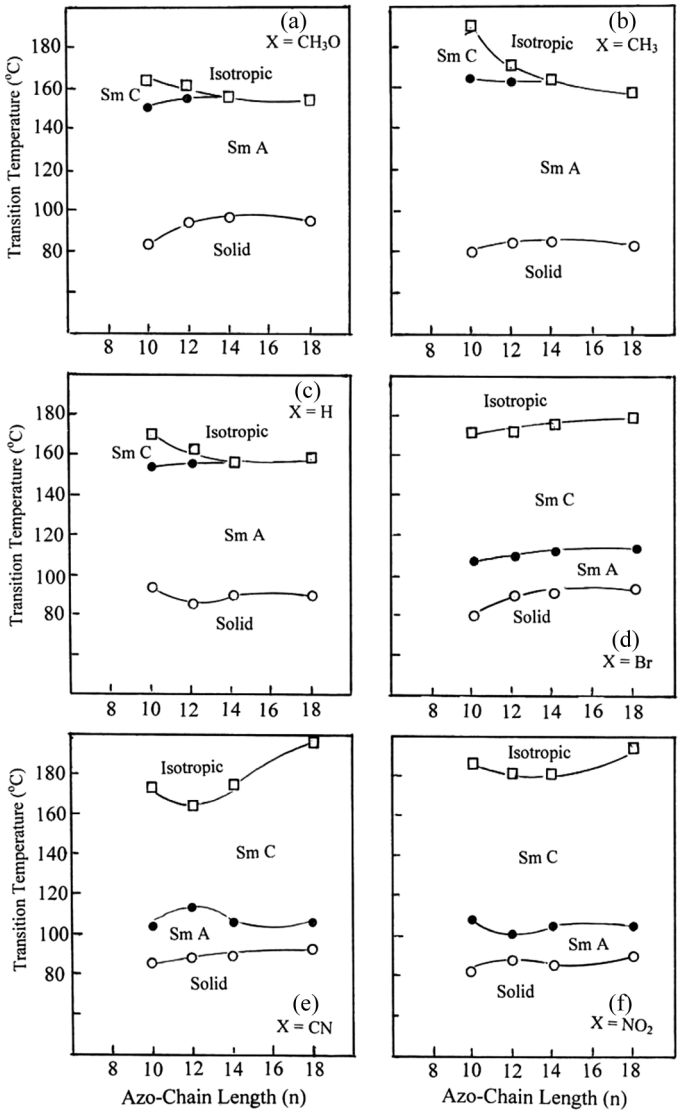

FIGURE 3 Effect of Azo-chain length (n) on the transition temperature of the supramolecular complexes of Group ***B*** series, (a) X = CH_3O, (b) X = CH_3, (c) X = H, (d) X = Br, (e) X = CN, and (f) X = NO_2.

the central part of the molecule. Of course, the terminal substituent can affect the polarizability of the aromatic rings to which they are attached; in addition, they may interact with the lateral portion of

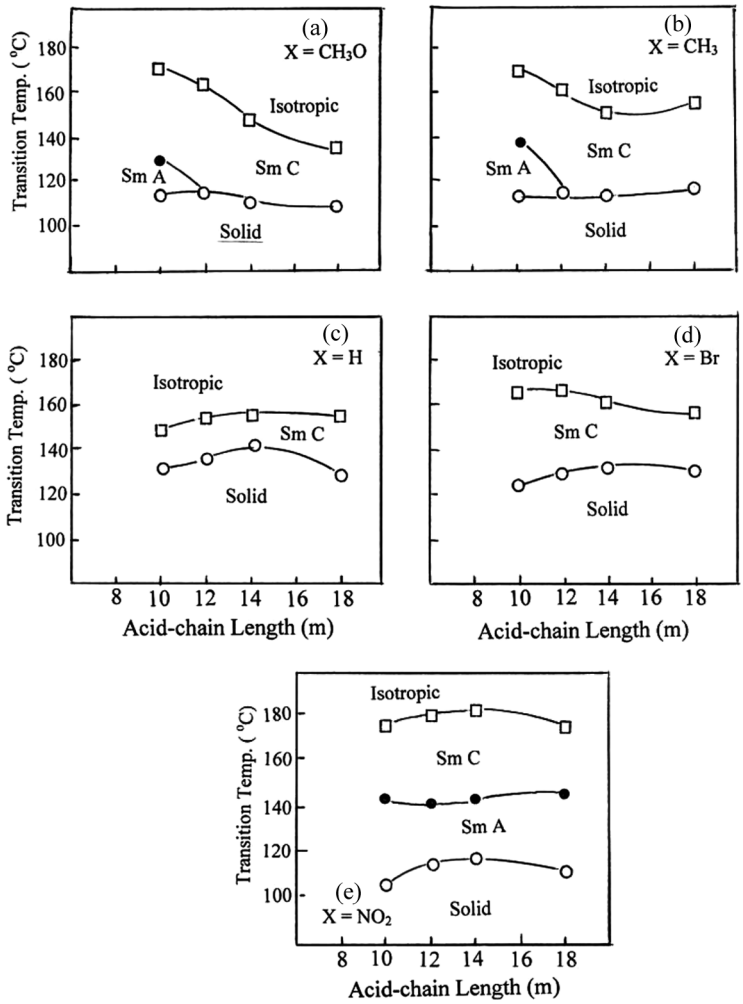

FIGURE 4 Effect of Acid-chain length (m) on the transition temperature of the supramolecular complexes of Group ***C*** series, (a) X = CH_3O, (b) X = CH_3, (c) X = H, (d) X = Br, (e) X = NO_2.

an adjacent molecule. As the polarity of the group decreases, the clearing temperature ($\boldsymbol{T}_C$) seems to be lowered too. This was attributed [15] to increased intermolecular attractions as the polarity and polarizability of the substituent are increased. Van der Veen [16] has deduced an equation that relates the mesophase-isotropic transition temperatures ($\boldsymbol{T}_C$) to the polarizability anisotropy ($\Delta\alpha_x$) of

the bonds C_{Ar}-X to small compact substituents. The relation has the formula

$$T_C \quad \alpha(\Delta\alpha_M + \Delta\alpha_x)^2, \tag{1}$$

where T_C is measured in Kelvin. The term $\Delta\alpha_M$ is the polarizability anisotropy for all the molecular structures except the terminal substituent, X. Equation (1) can be put in the following form

$$\sqrt{T}_C = a \cdot \Delta\alpha_M + a \cdot \Delta\alpha_X, \tag{2}$$

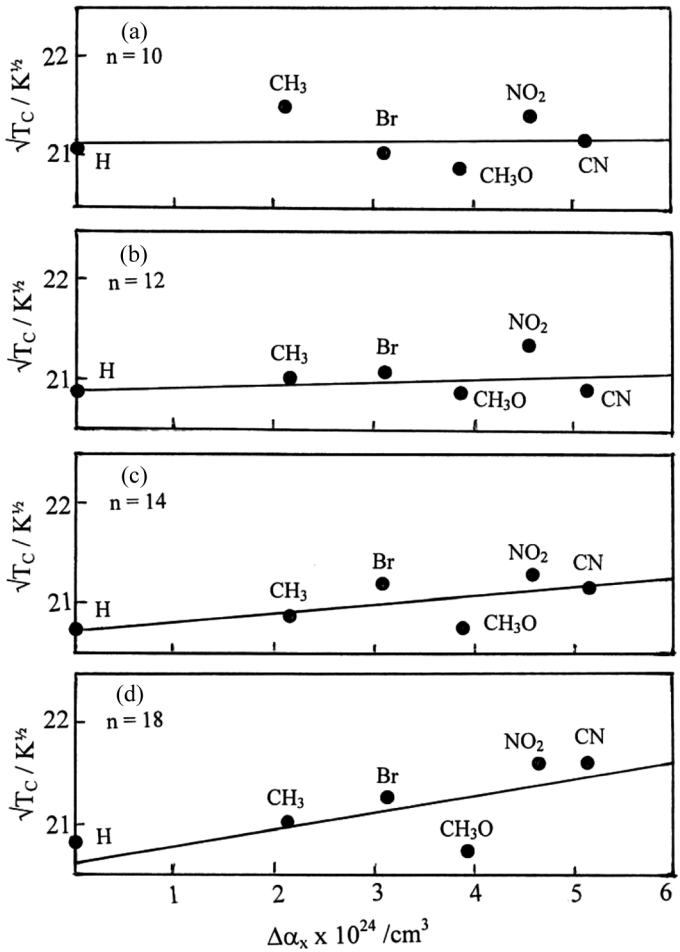

FIGURE 5 Dependence of the $\sqrt{T}_C$ of the supramolecular complexes of Group ***B*** series on the polarizability anisotropy, $\Delta\alpha_X$, of the polar substituent, X.

where "a" is the proportionality constant. The polarizability anisotropy, $\Delta\alpha_X$, of the various C_{Ar}-X bonds was calculated using the data of LeFevre and coworkers [17–19] and the values are included in Table 6. Thus, if $\sqrt{T_C}$ is plotted against $\Delta\alpha_X$ for the two series of liquid crystalline complexes (groups ***B*** and ***C***), a straight line is expected, the slope of which equals "a" and the intercept equals "$a \cdot \Delta\alpha_M$." The $\sqrt{T_C}$ values for group ***B*** series were plotted as a function of $\Delta\alpha_X$ and the plots are depicted in Fig. 5.

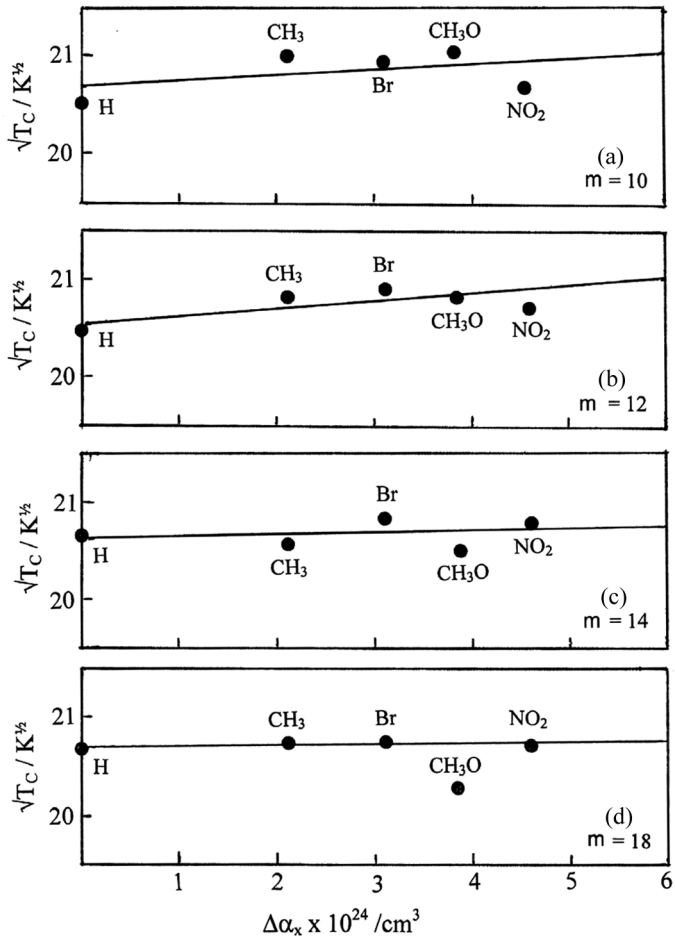

FIGURE 6 Dependence of the $\sqrt{T_C}$ of the supramolecular complexes of Group ***C*** series on the polarizability anisotropy, $\Delta\alpha_X$, of the polar substituent, X.

TABLE 7 Van der Veen Data for the Two Series ***B*** and ***C***

Series	n or m	Slope "a" $\times 10^{-22}$	Intercept ($a\Delta\alpha_M$)
Group ***B***	10	0.80	21.14
	12	2.68	20.90
	14	9.28	20.69
	18	16.69	20.59
Group ***C***	10	6.20	20.68
	12	8.21	20.55
	14	1.45	20.68
	18	≈ 0	20.73

For the sake of comparison, the corresponding data for the supramolecular hydrogen-bonded liquid crystals previously investigated (group ***C***) are similarly plotted in Fig. 6.

Applying the method of least squares using Eq. (2) on all the regression data in Figs. 5 and 6, the corresponding "a and $\Delta\alpha_M$" for each group of data and the results are collected in False Table 7. These results revealed that the slopes "a" in both series are generally small, indicating that substitution, whether in the pyridine-based constituent or in the acid partner, is poor in promoting stability to the mesophase induced by the hydrogen-bond within the complex. Nevertheless, comparing the values of any two corresponding data in the two series (***B*** and **C**) revealed that the slopes are somewhat greater when substituent X is in the pyridine-based portion and the alkoxy chain in the acid is short (n or $m = 10$ and 12). The reverse holds good for the higher two homologues (n or $m = 14$ and 18). It is worth remembering here that any two corresponding members in the two series (***B*** and ***C***) the first is produced by the exchange of the two terminal substituents, X- and -OR (compare series **B** and **C**).

CONCLUSIONS

Four pyridine-based azo dye derivatives of the type 4-(4′-pyridylazo phenyl)-4″-alkoxy benzoates, **I***10*–**I***18*, in which the alkoxy chain length varies between 10 and 18 carbons, respectively, were prepared and investigated for their mesophase behavior. Three groups of supramolecular complexes, having in common, the 4-pyridylazo phenyl benzoate/benzoic acid core, were investigated via differential scanning calorimetry (DSC) and polarized-light microscopy (PLM). In the first (group **A**), each of the pyridine-based and benzoic acid portions of the complexes carries an alkoxy group of varying chain length. In

the second (group **B**), a polar substituent (X) is introduced to the acid portion while an alkoxy group, again of varying chain length, is alternatively attached to the pyridine-based moiety. A reversed substitution, to that in group ***B*** was realized in group ***C***.

The study revealed that:

1. The Sm C mesophase is induced in all cases, irrespective of the polarity of the substituent X or the length of the alkoxy group.
2. Increasing the alkoxy chain length, either in the pyridine-based or benzoic acid moieties, enhances the Sm C mesophase to the extent that it stands as the only mesophase when m or $n = 18$ carbons.
3. The effect of the polar substituent X on the stability of the Sm C phase is more pronounced when it is on the pyridine-based moiety and the chain on the acid is short ($m = 10$ or 12). Conversely, for longer alkoxy chain, the Sm C stability is enhanced when the substituent X is on the acid partner.

REFERENCES

[1] Pelzl, G., Demus, D., & Sackmann, H. (1968). *Z. Phys. Chem.*, *238*, 22.
[2] Revannasiddaiah, N. D. & Krishnamurti, D. (1983). *Mol. Cryst. Liq. Cryst.*, *101*, 103.
[3] Bengs, H., Ebert, M., Karthaus, O., Kohne, B., Praefcke, K., Ringsdorf, H., Wendorf, J. H., & Wustefeld, R. (1990). *Adv. Mater.*, *2*, 141.
[4] Praefcke, K., Singer, D., Kohne, B., Ebert, M., Liebmann, A., & Wendorf, J. H. (1991). *Liq. Cryst.*, *10*, 147.
[5] Bengs, H., Karthaus, O., Ringsdorf, H., Baehr, C., Ebert, M., & Wendorf, J. H. (1991). *Liq. Cryst.*, *10*, 161.
[6] Praefcke, K., Singer, D., Langner, M., Kohne, B., Ebert, M., Liebmann, A., & Wendorf, J. H. (1992). *Mol. Cryst. Liq. Cryst.*, *215*, 121.
[7] Praefcke, K. & Holberg, J. D. (1996). *J. Incl. Phen. Mol. Recog. Chem.*, *24*, 19.
[8] Paleos, C. M. & Tsiourvas, D. (1995). *Angew. Chem. Int. Ed. Engl.*, *24*, 1696.
[9] Paleos, C. M. & Tsiourvas, D. (2001). *Liq. Cryst.*, *28*, 1127.
[10] Prade, H., Miethchen, R., & Vill, V. (1995). *J. Prkt. Chem.*, *337*, 427.
[11] Naoum, M. M., Fahmi, A. A., & Alaasar, M. A. (2008). *Mol. Cryst. Liq. Cryst.*, *482*, 57.
[12] Naoum, M. M., Saad, G. R., Nessim, R. I., Abdel Aziz, T. A., & Seliger, H. (1997). *Liq. Cryst.*, *23*, 789.
[13] Song, X., Li, J., & Zhang, S. (2003). *Liq. Cryst.*, *30*, 331.
[14] Cammenga, H. K., Eysel, W., Gmelin, E., Hemmiger, W., Hoehne, G. W. H., & Sagre, S. M. (1993). *Thermochim. Acta*, *219*, 333.
[15] Schroeder, J. P. & Bristol, D. W. (1973). *J. Org. Chem.*, *38*, 3160; Schroeder, J. P. & Bristol, D. W. (1970). *J. Org. Chem.*, *35*, 3160.
[16] van der veen, J. (1975). *J. Phys., Colluque C1*, *36*, 375.
[17] Le Fevre, R. J. W. & Rao, B. P. (1958). *J. Chem. Soc. B.*, 1465.
[18] Aroney, M. J., Calderbank, K. E., Le Fevre, R. J. W., & Pierens, R. K. (1969). *J. Chem. Soc. B.*, 159.
[19] Aroney, M. J., Le Fevre, R. J. W., Pierens, R. K., & Mida, G. N., (1969). *The, J. Chem. Soc. B.*, 666.